Unambiguous and robust formulation for Wannier localization

Kangbo Li [1] Hsin-Yu Ko [2] Robert A. DiStasio, Jr. [2,*] and Anil Damle [1,†]

[1]*Department of Computer Science, Cornell University, Ithaca, New York 14853, USA*
[2]*Department of Chemistry and Chemical Biology, Cornell University, Ithaca, New York 14853, USA*

We provide a new variational definition for the spread of an orbital under periodic boundary conditions (PBCs) that is continuous with respect to the gauge, consistent in the thermodynamic limit, well suited to diffuse orbitals, and systematically adaptable to schemes computing localized Wannier functions. Existing definitions do not satisfy all these desiderata, partly because they depend on an "orbital center"—an ill-defined concept under PBCs. Based on this theoretical development, we showcase a robust and efficient ($10\times$–$70\times$ fewer iterations) localization scheme across a range of materials.

I. INTRODUCTION

Localized Wannier functions (LWFs) offer several theoretical and computational advantages over Bloch orbitals in condensed-phase electronic structure calculations. For instance, LWFs allow one to probe/characterize the local electronic structure in complex extended systems, thereby enabling chemical bonding analysis (e.g., floating bonds in amorphous Si [1,2]), orbital partitioning (e.g., computing molecular dipole moments in liquid water [3]), and chemical-environment-based features/targets for machine learning (ML) [4]. LWFs also play a critical role in evaluating the bulk properties of materials (e.g., in the modern theory of polarization [5–8] and magnetization [9–13]), predicting and understanding the spectroscopic signatures of condensed matter (e.g., IR [14] and Raman spectra [15]), as well as constructing effective model Hamiltonians (e.g., for quantum transport of electrons [16,17] and strongly correlated systems [18–21]). Computationally, LWFs enable large-scale electronic structure calculations to exploit the real-space sparsity (or "near sightedness" [22]) of exchange-correlation interactions (e.g., in hybrid density functional theory [23,24] and GW [25]). As such, a well-defined, robust, and efficient framework for computing LWFs is highly desirable.

In this work, we address two fundamental problems with existing methodologies for obtaining LWFs—one theoretical and one practical. On the theoretical side, we present an unambiguous ground-truth definition for the spread of an orbital under PBCs that has several favorable properties: continuity with respect to gauge transforms, consistency in the thermodynamic limit, and suitability for diffuse orbitals. Most importantly, this variational definition sidesteps the fundamentally ill-posed problem of determining an orbital center under PBCs, thereby yielding a gauge-continuous formulation well suited for generating LWFs. In contrast, prior work

based on adaptations of $\langle r^2 \rangle - \langle r \rangle^2$ (e.g., Marzari–Vanderbilt [26]) suffer from the inherent complexities associated with position operators in periodic systems (as studied by Resta [27,28]), and result in orbital spread ansatz that are not gauge continuous. Given the importance of computing LWFs, many alternative (and practically effective) expressions for orbital spread have been proposed [2,29–33]. While often deemed "equivalent" [34,35], we will show this is not the case.

Based on this theoretical development, we derive a systematic approximation to our ground-truth orbital spread definition that is local in **k** space and forms the basis for a robust and efficient scheme for generating LWFs. In practice, we show that our scheme consistently converges in at least an order-of-magnitude fewer iterations ($10\times$–$70\times$) than the widely used `Wannier90` code [36] across a diverse range of materials. The theoretical and practical contributions herein provide a strong foundation for automated LWF construction in large-scale systems across physics, chemistry, and materials science, and will thereby enable next-generation capabilities in the screening, discovery, and design of novel materials; characterization and analysis of complex multiscale systems; and generation of high-quality ML data at scale.

II. THEORY

Our definition for the spread of an orbital under PBCs is motivated by the variational characterization of the center of an orbital under open boundary conditions:

$$\mathbf{c}^* \triangleq \mathrm{argmin}_{\mathbf{r}'} \int \rho(\mathbf{r})(\mathbf{r} - \mathbf{r}')^2 \, d\mathbf{r} = \int \rho(\mathbf{r}) \, \mathbf{r} \, d\mathbf{r}, \qquad (1)$$

where $\rho(\mathbf{r})$ is the density of a Wannier function [37]. Adapting (1) for periodic systems leads to the density convolution (DC), denoted by $(\mathcal{S}\rho)$:

$$(\mathcal{S}\rho)(\mathbf{r}') \triangleq \int_{\mathbb{S}_{\mathbf{r}'}} \rho(\mathbf{r})(\mathbf{r} - \mathbf{r}')^2 \, d\mathbf{r}$$

$$= \int_{\mathbb{S}_0} \rho(\mathbf{r} + \mathbf{r}') \, \mathbf{r}^2 \, d\mathbf{r}, \qquad (2)$$

*Contact author: distasio@cornell.edu
†Contact author: damle@cornell.edu
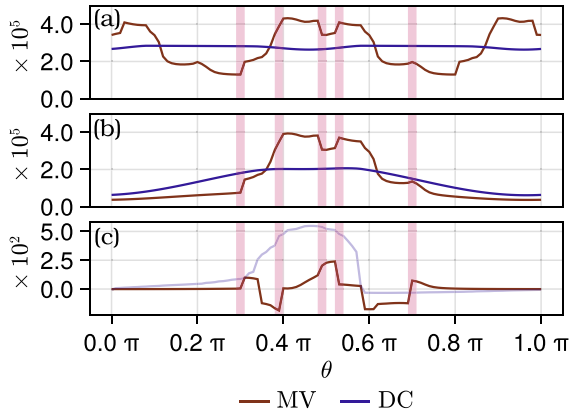
FIG. 1. Variation of (a) sum of spreads of $|1\rangle$ and $|2\rangle$, (b) spread of $|1\rangle$, and (c) center of $|1\rangle$ with respect to the gauge, $U(\theta)$, for a 1D periodic system containing two Wannier functions ($|1\rangle$, $|2\rangle$) [37]. While s_{DC} is continuous with respect to the (π-periodic) gauge, s_{MV} is not; also highlighted are some of the discontinuities of s_{MV} and $\mathbf{c}_{MV}$.

where $\mathbb{S}_0$ is the Born-von Karman supercell (i.e., the unit cell replicated with respect to the $\mathbf{k}$-point mesh) and $\mathbb{S}_{\mathbf{r}'}$ is the supercell translated by $\mathbf{r}'$. The corresponding DC center ($\mathbf{c}_{DC}$) and DC spread (s_{DC}) are then defined as the minimizer and minimum of (2):

$$\mathbf{c}_{DC} \triangleq \operatorname{argmin}_{\mathbf{r}'} (\mathcal{S}\rho)(\mathbf{r}'), \tag{3}$$

$$s_{DC} \triangleq \min_{\mathbf{r}'} (\mathcal{S}\rho)(\mathbf{r}'). \tag{4}$$

A key feature of s_{DC} is continuity with respect to the gauge chosen for the Wannier functions. This property arises because s_{DC} is explicitly defined as the minimum of an optimization problem—a continuous quantity with respect to the gauge in this case. This is in stark contrast to commonly used orbital spread definitions based on $\langle r^2 \rangle - \langle r \rangle^2$ (e.g., [26]) that can be discontinuous with respect to the gauge—a property inherited from explicitly depending on the ill-defined notion of an orbital center under PBCs [27,28]. We sidestep this issue by using a center-independent formulation [cf. (4)]; hence, the fact that $\mathbf{c}_{DC}$ is not necessarily continuous with respect to the gauge (as the periodicity implies multiple minimizers) cannot plague s_{DC} even though $s_{DC} = (\mathcal{S}\rho)(\mathbf{c}_{DC})$ for any $\mathbf{c}_{DC}$ satisfying (3).

To illustrate this advantage, Fig. 1 shows how s_{DC} varies with respect to the gauge for a two-state system [37]. For comparison, we also consider the Marzari-Vanderbilt (MV) spread (s_{MV}) [26], the optimization of which leads to the so-called maximally localized Wannier functions (MLWFs). Figures 1(a) and 1(b) show that s_{MV} is discontinuous with respect to the gauge, as is $\mathbf{c}_{MV}$ [Fig. 1(c)]. In contrast, s_{DC} is a smooth function of the gauge even though $\mathbf{c}_{DC}$ is ill behaved.

The DC formulation in (3) and (4) can be intuitively thought of as implicitly using the optimal integration boundary when computing an orbital spread in real space. Moreover, numerical evaluation of the underlying DC integral in (2) (e.g., via a Fourier transform) corresponds to a spectrally accurate computation of the orbital spread. Hence, the DC formulation is both consistent in the thermodynamic limit and more accurate for finite-sized domains than common
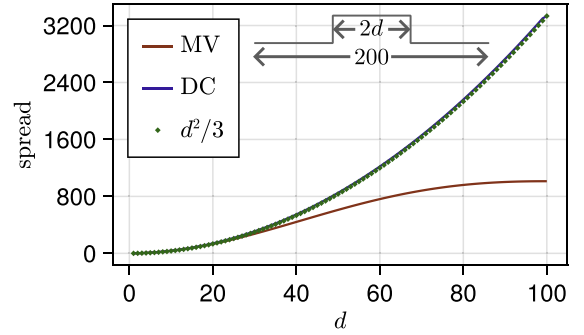
FIG. 2. Spread of a square wave in a 1D periodic domain $[-100, 100)$ as a function of the width $2d$. s_{DC} captures the expected $d^2/3$ behavior while s_{MV} only does so when d is small relative to the domain.

first-order expressions (i.e., as used explicitly by Marzari and Vanderbilt [26] via a finite-difference scheme and implicitly by Resta [27] via the use of a single low-frequency Fourier mode when defining the position operator). Accordingly, s_{DC} is better suited to quantifying the spread of diffuse orbitals (relative to the unit cell) as well as orbitals centered near unit-cell boundaries. To concretely illustrate the validity of s_{DC} for both local and diffuse orbitals, Fig. 2 considers the spread of a square wave (width $= 2d$) in a 1D periodic domain. While s_{DC} gives the exact spread ($d^2/3$), s_{MV} is only accurate when d is small relative to the domain and becomes increasingly inaccurate as d grows. This discrepancy can also be seen in real systems, e.g., a K-doped molten KCl salt ($K_{33}Cl_{31}$) [38–41], in which the bipolaron state is close to the conduction band and quite diffuse. Figure 3 clearly shows that s_{MV} deviates from the ground truth s_{DC} as the orbitals become more
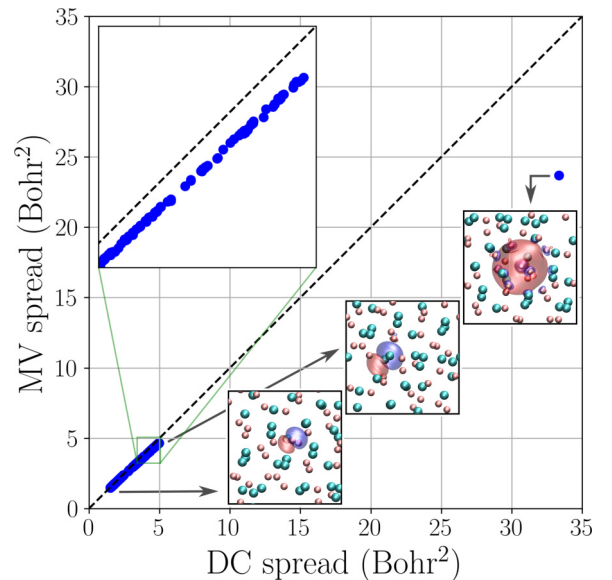
FIG. 3. Comparison of s_{DC} and s_{MV} for the LWFs in $K_{33}Cl_{31}$ computed with `Wannier90` (blue dots). As the orbitals become more diffuse, s_{MV} deviates significantly from the ground truth s_{DC}. Insets show select orbital isosurfaces (± 0.0001) overlaid with the unit cell (simple cubic; side length 26.59 Bohr; [41]).

diffuse—in this case, severely underestimating the spread of the bipolaron state by roughly 30%.

One of the most practical and prominent uses for an orbital spread expression is within iterative methods for Wannier localization [34]. While (4) can easily be computed given an orbital density, s_{DC} is cumbersome to optimize directly since (2) is a nonlocal operator in $\mathbf{k}$ space. Hence, we now derive a systematic approximation to s_{DC} that is center independent, gauge continuous, and consistent in the thermodynamic limit. Moreover, it can be used as a surrogate for s_{DC} within optimization schemes for computing LWFs, and, if desired, s_{DC} can be computed for the converged orbitals.

Our derivation [37] starts with the truncated cosine approximation

$$\mathbf{r}^2 \gtrapprox \sum_{\mathbf{b}} 2\, w_{\mathbf{b}} \Re\left(1 - e^{-i\,\mathbf{b}^T \mathbf{r}}\right), \tag{5}$$

where $\mathbf{b}$ are selected nearest-neighbor vectors and $w_{\mathbf{b}}$ are the associated weights [26]. This leads to the (often tight) lower bound

$$(\mathcal{S}\rho)(\mathbf{r}') \gtrapprox \sum_{\mathbf{b}} 2\, w_{\mathbf{b}} \Re\left(1 - \hat{\rho}(\mathbf{b})\, e^{i\,\mathbf{b}^T \mathbf{r}'}\right), \tag{6}$$

where $\hat{\rho}(\mathbf{b}) = \int_{\mathbb{S}_0} \rho(\mathbf{r})\, e^{-i\,\mathbf{b}^T \mathbf{r}}\, d\mathbf{r}$ is the unnormalized Fourier transform of $\rho(\mathbf{r})$. For the nth Wannier function, $\hat{\rho}(\mathbf{b}) = \frac{1}{N} \sum_{\mathbf{k}} M_{n,n}^{\mathbf{k},\mathbf{k}+\mathbf{b}}$, wherein N is the number of electrons and M is the set of $\mathbf{k}$-space overlap matrices [26]. Minimizing the right hand side of (6) by choosing $\mathbf{r}'$ to eliminate the phase of $\hat{\rho}(\mathbf{b})$ yields

$$s_{DC} \gtrapprox s_{TDC} \triangleq \sum_{\mathbf{b}} 2\, w_{\mathbf{b}}(1 - |\hat{\rho}(\mathbf{b})|), \tag{7}$$

where s_{TDC} is the truncated DC (TDC) approximation and a formal lower bound to s_{DC}. In contrast, s_{MV} can either overestimate or underestimate s_{DC} (Fig. 1). Importantly, s_{TDC} retains the center independence of s_{DC}; since $\hat{\rho}(\mathbf{b})$ is continuous with respect to the gauge, this implies that s_{TDC} is also gauge continuous (Fig. S1 [37]). Like s_{DC}, s_{TDC} can be seamlessly applied to both Γ-point and $\mathbf{k}$-point calculations without modification.

Interestingly, a Γ-point only version of s_{TDC} was heuristically proposed in Berghold *et al.* [29] (by extension of Ref. [33]); Stengel and Spaldin [32] built off this work to compute orbital centers for polarization. However, Berghold *et al.* [29] focused on numerical agreement of several orbital spread ansatz for a fixed gauge, rather than their behavior with respect to changes in the gauge; hence, these alternative expressions were deemed (essentially) equivalent to s_{MV} [29,34,35]. In contrast, we rigorously derive (7) from our DC formulation and demonstrate that s_{TDC} has clear theoretical and practical advantages over s_{MV}: it is a center-independent and gauge-continuous definition of orbital spread (*vide supra*) that yields a robust and efficient scheme for computing LWFs (*vide infra*).

III. COMPUTATIONAL RESULTS

To highlight the sizable improvements provided by s_{TDC} during iterative localization, we computed LWFs for a suite of materials using an in-house version of our code [42]
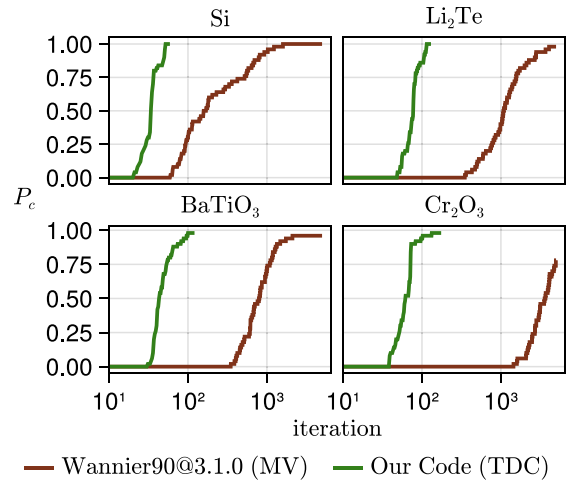
FIG. 4. Fraction of orbital localization computations P_c that reached success within a given number of iterations for four materials. Using an s_{TDC}-based (vs. an s_{MV}-based) objective function consistently provided an order-of-magnitude ($10\times$–$70\times$) reduction in the number of iterations needed to achieve success.

and `Wannier90` (v3.1.0) [36]. At its core, our code implements the same gradient-based optimization algorithm as `Wannier90`, but uses s_{TDC} (instead of s_{MV}) to define the objective function (i.e., as the sum over orbital spreads). Notably, the favorable properties of the TDC scheme allowed for a comparatively simple implementation of manifold optimization paired with standard criteria to reliably determine convergence.

To compare the convergence behavior of objective functions based on s_{TDC} and s_{MV}, we considered four materials with diverse bonding types: Si, Li_2Te, $BaTiO_3$, and Cr_2O_3 [37]. We performed a series of 50 iterative localization computations per material, each starting from a different randomly generated gauge [43]. Figure 4 characterizes the convergence behavior by plotting the fraction of computations P_c that succeeded within a given number of iterations (with success defined retrospectively as reaching within 0.1% of the minimum objective value achieved across all 50 runs). Using s_{TDC} consistently provided an order-of-magnitude reduction in the number of iterations required to achieve success relative to s_{MV} (i.e., typically $10\times$–$70\times$ fewer iterations for a fixed P_c) [44]. Our s_{TDC}-based code is robust and converged for all 200 runs. Moreover, it did not achieve success only twice (once each for $BaTiO_3$ and Cr_2O_3), indicating that suboptimal local minima are—in contrary to common belief—likely rare for these non-trivial systems. All `Wannier90` computations were run for 5000 iterations, with P_c evaluated by retrospectively determining the first iteration that achieved success during each run. Even with this favorable criteria, `Wannier90` computations often failed—e.g., for Cr_2O_3, success was never achieved within 1000 iterations and $P_c \approx 0.75$ after 5000 iterations [44].

To better understand the convergence behavior in Fig. 4, Fig. 5 considers a pair of successful localization computations for Si. Figure 5(a) shows that s_{MV} for the highlighted orbital was not monotonic during the `Wannier90` optimization trajectory (e.g., iterations 250–300). Such behavior implies that
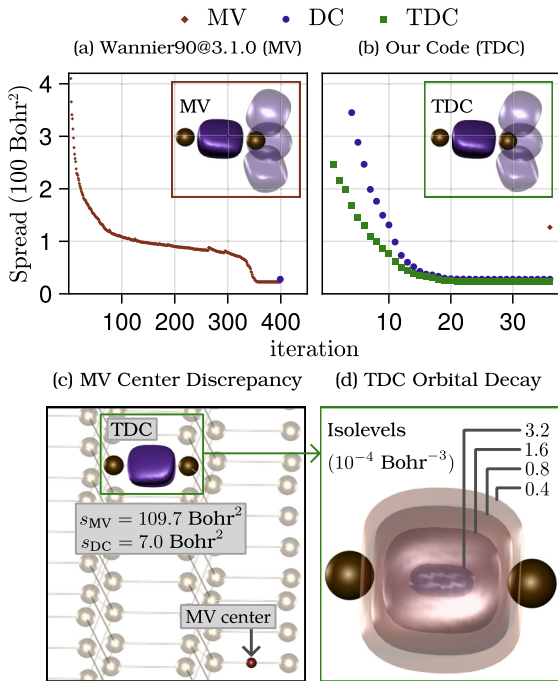
FIG. 5. Characterization of two successful localization computations for Si from Fig. 4. (a) Nonmonotonic decay of s_{MV} for the highlighted orbital computed with `Wannier90` (see inset). (b) Evolution of s_{TDC} for the analogous orbital computed with our code, which achieves success in $\approx 10\times$ fewer iterations; s_{MV} severely overestimates the spread of this orbital. (c) Distant location of $\mathbf{c}_{MV}$ leads to the large discrepancy between s_{MV} and s_{TDC} (or s_{DC}) for the highlighted orbital in (b). (d) Orbital isosurfaces depict the expected (approximate) exponential decay of the highlighted orbital in (b) and (c).

`Wannier90` encountered (and "escaped" from) potentially suboptimal local minima, consistent with Cancès *et al.* [45]; further investigation suggests these might be nondifferentiable (i.e., nonsmooth) points where the "gradient" (as defined by the standard MV formulation) is nonvanishing—a challenging scenario for any optimizer. In contrast, Fig. 5(b) shows that s_{TDC} for the analogous orbital monotonically decreases when optimized using our code, which reaches the same LWFs (per a visual metric) as `Wannier90` in an order-of-magnitude

fewer iterations. Matching theoretical expectations, s_{TDC} lower bounds s_{DC} and the metrics converge as the orbital becomes more localized. However, s_{MV} severely overestimates the spread of the highlighted LWF computed using our s_{TDC}-based code. This discrepancy stems from the distant location of $\mathbf{c}_{MV}$ shown in Fig. 5(c)—highlighting a potential danger of center-based definitions like s_{MV}. Consistent with both s_{TDC} and s_{DC}, Fig. 5(d) confirms that the LWF computed using our code exhibits exponential decay. While s_{MV} can sometimes fail to recognize localized orbitals [cf. Figs. 5(b)–5(d)], s_{TDC}—by construction—is not prone to such issues.

IV. CONCLUSIONS

By providing an unambiguous ground-truth definition for orbital spread and a corresponding robust scheme for generating LWFs in complex systems with unprecedented efficiency, this work addresses key theoretical and practical issues that currently limit the use of LWFs in next-generation applications. These contributions enable fully autonomous construction of LWFs in diverse and large-scale systems, paving the way for state-of-the-art materials discovery and physics-informed ML at scale. While we only discussed insulating systems, entangled systems can also be treated by adapting Ref. [46] to use s_{TDC}—an interesting future research direction. Accompanying this article are two Julia packages [42] that allow researchers to experiment with and expand upon our work.

[1] M. Fornari, N. Marzari, M. Peressi, and A. Baldereschi, Comput. Mater. Sci. **20**, 337 (2001).

[2] P. L. Silvestrelli, N. Marzari, D. Vanderbilt, and M. Parrinello, Solid State Commun. **107**, 7 (1998).

[3] P. L. Silvestrelli and M. Parrinello, Phys. Rev. Lett. **82**, 3308 (1999).

[4] L. Zhang, M. Chen, X. Wu, H. Wang, W. E, and R. Car, Phys. Rev. B **102**, 041121(R) (2020).

[5] R. Resta, Ferroelectrics **136**, 51 (1992).

[6] R. Resta, Rev. Mod. Phys. **66**, 899 (1994).

[7] R. D. King-Smith and D. Vanderbilt, Phys. Rev. B **47**, 1651 (1993).

[8] D. Vanderbilt and R. D. King-Smith, Phys. Rev. B **48**, 4442 (1993).

[9] T. Thonhauser, D. Ceresoli, D. Vanderbilt, and R. Resta, Phys. Rev. Lett. **95**, 137205 (2005).

[10] D. Xiao, J. Shi, and Q. Niu, Phys. Rev. Lett. **95**, 137204 (2005).

[11] D. Ceresoli, T. Thonhauser, D. Vanderbilt, and R. Resta, Phys. Rev. B **74**, 024408 (2006).

[12] J. Shi, G. Vignale, D. Xiao, and Q. Niu, Phys. Rev. Lett. **99**, 197202 (2007).

[13] I. Souza and D. Vanderbilt, Phys. Rev. B **77**, 054438 (2008).

[14] M. Sharma, R. Resta, and R. Car, Phys. Rev. Lett. **95**, 187401 (2005).

[15] Q. Wan, L. Spanu, G. A. Galli, and F. Gygi, J. Chem. Theory Comput. **9**, 4124 (2013).

[16] A. Calzolari, N. Marzari, I. Souza, and M. B. Nardelli, Phys. Rev. B **69**, 035108 (2004).

[17] Y.-S. Lee, M. B. Nardelli, and N. Marzari, Phys. Rev. Lett. **95**, 076804 (2005).

[18] S. Fabris, S. de Gironcoli, S. Baroni, G. Vicario, and G. Balducci, Phys. Rev. B **71**, 041102(R) (2005).

[19] V. I. Anisimov, A. V. Kozhevnikov, M. A. Korotin, A. V. Lukoyanov, and D. A. Khafizullin, J. Phys.: Condens. Matter **19**, 106206 (2007).

[20] T. Miyake and F. Aryasetiawan, Phys. Rev. B **77**, 085122 (2008).

[21] P. Umari, G. Stenuit, and S. Baroni, Phys. Rev. B **79**, 201104(R) (2009).

[22] E. Prodan and W. Kohn, Proc. Natl. Acad. Sci. USA **102**, 11635 (2005).

[23] H.-Y. Ko, J. Jia, B. Santra, X. Wu, R. Car, and R. A. DiStasio, Jr., J. Chem. Theory Comput. **16**, 3757 (2020).

[24] H.-Y. Ko, B. Santra, and R. A. DiStasio, Jr., J. Chem. Theory Comput. **17**, 7789 (2021).

[25] C. Buth, U. Birkenheuer, M. Albrecht, and P. Fulde, Phys. Rev. B **72**, 195107 (2005).

[26] N. Marzari and D. Vanderbilt, Phys. Rev. B **56**, 12847 (1997).

[27] R. Resta, Phys. Rev. Lett. **80**, 1800 (1998).

[28] R. Resta, J. Phys.: Condens. Matter **22**, 123201 (2010).

[29] G. Berghold, C. J. Mundy, A. H. Romero, J. Hutter, and M. Parrinello, Phys. Rev. B **61**, 10040 (2000).

[30] K. S. Thygesen, L. B. Hansen, and K. W. Jacobsen, Phys. Rev. B **72**, 125119 (2005).

[31] P. L. Silvestrelli, Phys. Rev. B **59**, 9703 (1999).

[32] M. Stengel and N. A. Spaldin, Phys. Rev. B **73**, 075121 (2006).

[33] R. Resta and S. Sorella, Phys. Rev. Lett. **82**, 370 (1999).

[34] N. Marzari, A. A. Mostofi, J. R. Yates, I. Souza, and D. Vanderbilt, Rev. Mod. Phys. **84**, 1419 (2012).

[35] P. F. Fontana, A. H. Larsen, T. Olsen, and K. S. Thygesen, Phys. Rev. B **104**, 125140 (2021).

[36] G. Pizzi, V. Vitale, R. Arita, S. Blügel, F. Freimuth, G. Géranton, M. Gibertini, D. Gresch, C. Johnson, T. Koretsune, J. Ibañez Azpiroz, H. Lee, J.-M. Lihm, D. Marchand, A. Marrazzo, Y. Mokrousov, J. I. Mustafa, Y. Nohara, Y. Nomura, L. Paulatto *et al.*, J. Phys.: Condens. Matter **32**, 165902 (2020).

[37] See Supplemental Material at http://link.aps.org/supplemental/10.1103/PhysRevB.110.085127 for more details on our derivations and experiments, which also includes Refs. [47–55].

[38] A. Selloni, P. Carnevali, R. Car, and M. Parrinello, Phys. Rev. Lett. **59**, 823 (1987).

[39] A. Selloni, R. Car, M. Parrinello, and P. Carnevali, J. Phys. Chem. **91**, 4947 (1987).

[40] E. S. Fois, A. Selloni, M. Parrinello, and R. Car, J. Phys. Chem. **92**, 3268 (1988).

[41] P. Pegolo, F. Grasselli, and S. Baroni, Phys. Rev. X **10**, 041031 (2020).

[42] Code available at https://github.com/kangboli/WTP.jl and https://github.com/kangboli/SCDM.jl.

[43] Using randomly projected *s*-orbitals in `Wannier90` did not meaningfully change its convergence behavior in Fig. 4.

[44] Using s_{DC} as an impartial adjudicator, we verified that the LWFs used to define success for each method had nearly identical spreads.

[45] E. Cancès, A. Levitt, G. Panati, and G. Stoltz, Phys. Rev. B **95**, 075114 (2017).

[46] A. Damle, A. Levitt, and L. Lin, Multiscale Model. Sim. **17**, 167 (2019).

[47] A. A. Mostofi, J. R. Yates, Y.-S. Lee, I. Souza, D. Vanderbilt, and N. Marzari, Comput. Phys. Commun. **178**, 685 (2008).

[48] P.-A. Absil, R. Mahony, and R. Sepulchre, *Optimization Algorithms on Matrix Manifolds* (Princeton University Press, Princeton, NJ USA, 2007).

[49] J. Hu, X. Liu, Z.-W. Wen, and Y.-X. Yuan, J. Operations Res. Soc. Chin. **8**, 199 (2020).

[50] R. Bergmann, J. Open Source Software **7**, 3866 (2022).

[51] T. Abrudan, J. Eriksson, and V. Koivunen, Signal Process. **89**, 1704 (2009).

[52] J. Manton, IEEE Trans. Signal Process. **50**, 635 (2002).

[53] A. Edelman, T. A. Arias, and S. T. Smith, SIAM J. Matrix Anal. Appl. **20**, 303 (1998).

[54] V. Vitale, G. Pizzi, A. Marrazzo, J. R. Yates, N. Marzari, and A. A. Mostofi, npj Comput. Mater. **6**, 66 (2020).

[55] A. Damle and L. Lin, Multiscale Model. Sim. **16**, 1392 (2018).